

# Optimizing chemistry of bulk metallic glasses for improved thermal stability

G S Dulikravich<sup>1</sup>, I N Egorov<sup>2</sup> and M J Colaco<sup>3</sup>

<sup>1</sup> Department of Mechanical and Materials Engineering, EC 3474, MAIDROC Lab., Florida International University, College of Engineering and Computing, 10555 West Flagler Street, Miami, Florida 33174, USA

<sup>2</sup> IOSO Technology Center; Milashenkova Ulitsa 10-201, Moscow 127322, Russia

<sup>3</sup> Department of Mechanical and Materials Engineering (DE/4), Military Institute of Eng. (IME), Praca General Tiburcio, 80, Rio de Janeiro, RJ 22290-270, Brazil

E-mail: [dulikrav@fiu.edu](mailto:dulikrav@fiu.edu), [egorov@iosotech.com](mailto:egorov@iosotech.com) and [colaco@ime.eb.br](mailto:colaco@ime.eb.br)

Received 2 December 2007, in final form 27 July 2008

Published 8 September 2008

Online at [stacks.iop.org/MSMSE/16/075010](http://stacks.iop.org/MSMSE/16/075010)

## Abstract

Thermo-mechanical-physical properties of bulk metallic glasses (BMGs) depend strongly on the concentrations of each of the chemical elements in a given alloy. The proposed methodology for simultaneously optimizing these multiple properties by accurately determining proper concentrations of each of the alloying elements is based on the use of computational algorithms rather than on traditional experimentation, expert experience and intuition. Specifically, the proposed BMG design method combines an advanced stochastic multi-objective evolutionary optimization algorithm based on self-adapting response surface methodology and an existing database of experimentally evaluated BMG properties. During the iterative computational design procedure, a relatively small number of new BMGs need to be manufactured and experimentally evaluated for their properties in order to continuously verify the accuracy of the entire design methodology. Concentrations of the most important alloying elements can be predicted so that new BMGs have multiple properties optimized in a Pareto sense. This design concept was verified for superalloys using strictly experimental data. Thus, the key innovation here lies in arriving at the BMG compositions which will have the highest glass forming ability by utilizing an advanced multi-objective optimization algorithm while requiring a minimum number of BMGs to be manufactured and tested in order to verify the predicted performance of the predicted BMG compositions.

## 1. Introduction

Metallic glasses are very special alloys whose alloying components are in an amorphous glassy state rather than forming a standard crystalline structure. Thus, metallic glasses have no grain structure implying no grain boundaries and no dislocations and stacking faults. They are

several times stronger than steel and considerably harder and more elastic [1]. Duwez and co-workers [2], when working on rapid solidification of Au–Si alloys in the 1960s, obtained the first metallic glasses by using extremely high cooling rates ( $\sim 10^5 \text{ K s}^{-1}$ ). However, extremely high cooling rates are possible to implement only if heat transfer during cooling is basically one-dimensional as is the case when creating melt-spun ribbons of thickness up to approximately  $100 \mu\text{m}$ . Since most of the industrial cast products are larger and truly three-dimensional, the challenge is to make these materials in the bulk form which necessitates a significantly lower cooling rate at the walls of a casting mold. Otherwise, extremely high cooling rates would create extremely high thermal stresses in the cast object resulting in multiple fractures. Drehman *et al* [3] in 1982 found that almost 5 mm thick castings can be made from the metallic glass of composition  $\text{Pd}_{40}\text{Ni}_{40}\text{P}_{20}$ . Kui *et al* [4] were able to use suitable cooling and increase the thickness of the metallic glass to more than 10 mm. Cooling rates of the newer alloys are from 100 to  $1 \text{ K s}^{-1}$  and the possible thickness of these newer metallic glasses increased from micrometers to a few centimeters. This gave rise to the possibility that metallic glasses can be manufactured in the bulk form if the alloying elements and their concentrations are chosen appropriately.

Due to the pioneering and systematic work of Inoue *et al* [4,5] in Japan since 1988, a large number of compositions have been discovered in the La, Zr, Pd, Mg, Fe based systems. Based on these results, Inoue had proposed three criteria for bulk metallic glass (BMG) formation.

1. Multi-component systems with more than three components. As the number of components increases, the number of possible phases that can nucleate from the melt increases. A somewhat naïve explanation was given that there is confusion in the melt as to which phase will nucleate first thus causing the melt to transform into glass. This is known as the *confusion principle*.
2. The difference between the radii of the atoms of the components should be more than 15%. This would ensure that crystalline solutions do not form.
3. Heat of mixing between the components should be negative. This would lead to intermetallic compound formation rather than cluster formation.

The glass forming ability (GFA) of an alloy melt can be judged by the difficulty in achieving the lowest possible cooling rate,  $R_c$ , at which the glass will still form. If critical cooling rates are lower, this means that thicker sections can be cast into glass, which implies a higher GFA.

Turnbull [3] suggested that a high reduced glass transition temperature,  $T_{rg}$ , defined as

$$T_{rg} = \frac{T_g}{T_m}, \quad (1)$$

where  $T_g$  is the glass transition at temperature and  $T_m$  is the melting (i.e. liquidus) temperature, is a good measure of GFA (figure 1). When a BMG is heated, it first undergoes structural relaxation where there is some rearrangement in atomic positions. Then, it undergoes a glass transition at temperature  $T_g$ , where its viscosity reduces drastically and it enters the super-cooled liquid region. At a slightly higher temperature,  $T_x$ , crystallization occurs by nucleation and growth of crystals.

Inoue *et al* [4,5] have shown that the width of the super-cooled liquid region given by

$$\Delta T_x = T_x - T_g \quad (2)$$

is also a good measure of GFA. The larger this temperature range of the super-cooled melt region, the higher the GFA. Figure 1 shows the relation between the cooling rate,  $R_c$ , and the two GFA parameters. It can be seen that systems having lower  $R_c$  have larger values for  $T_{rg}$  and  $\Delta T_x$ , but the scatter is less for  $\Delta T_x$ . Inoue's criterion is widely accepted by the BMG research community.

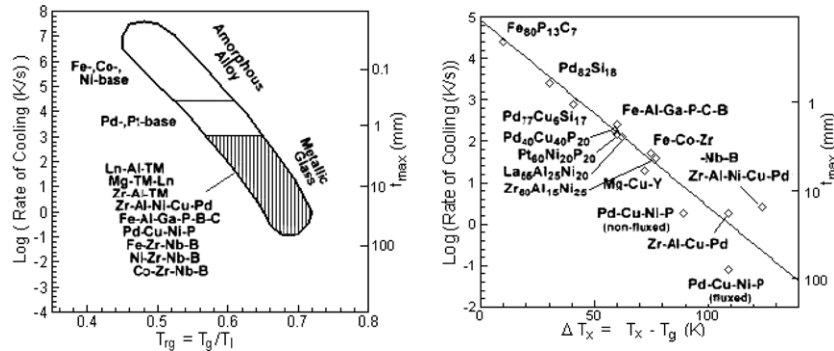


**Figure 1.** (a) Relationship between Turnbull's GFA criterion and critical cooling rate,  $R_c$ . (b) Relationship between Inoue's GFA criterion and critical cooling rate,  $R_c$ .

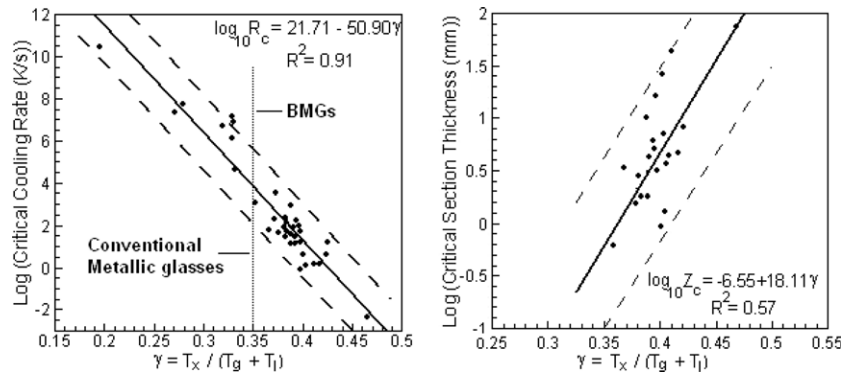


**Figure 2.** Variation of critical cooling rate,  $R_c$ , and critical section thickness,  $Z_c$ , as functions of Lu and Liu's GFA parameter,  $\gamma$ .

Recently, Fan *et al* [6] presented a novel formulation where an overestimation of GFA using  $T_{rg}$  can be corrected by introducing a new dimensionless  $\phi$  criterion, expressed by

$$\phi = T_{rg} \left( \frac{\Delta T_x}{T_g} \right)^a. \quad (3)$$

Here, exponent  $a = 0.143$ . Their published results of  $R_c$  versus  $\phi$  are superior to those of  $R_c$  versus  $T_{rg}$ .

Lu and Liu [7] have proposed yet another criterion for GFA defined as

$$\gamma = \frac{T_x}{T_g + T_l}, \quad (4)$$

where  $T_l$  is the liquidus temperature. Figure 2 shows the variation of  $R_c$  with  $\gamma$ . It can be seen that by increasing the value of  $\gamma$ , a lower cooling rate,  $R_c$ , is possible and consequently larger objects can be cast as BMGs [1].

There is also a growing need to minimize the number of highly expensive alloying components or their complete elimination by introducing some other alloying components [8] that could offer comparable multiple thermo-physical properties of the resulting BMGs.

Thus, the BMG design could have several simultaneous objectives. For example [1, 8–13]:

- maximize glass transition temperature,  $T_g$ ,
- maximize liquidus temperature,  $T_l$ ,

- maximize reduced glass transition temperature  $T_{rg} = T_g / T_1$ ,
- maximize the width of the super-cooled liquid region  $\Delta T_x = T_x - T_g$ ,
- maximize hardness,
- maximize Young's modulus,
- maximize density, and
- minimize cost of the raw material.

It should be immediately pointed out that brute-force optimization of thermo-mechanical properties of BMGs by varying chemical concentrations of  $N$  alloying elements is unfeasible. This approach to designing new classes of BMGs, that has not been attempted before, would involve creating an  $N$ -dimensional matrix of alloy compositions and then interpolating and searching for the extreme points in such a matrix. If the concentration of each alloying element is varied within its specified range, this variation could be approximated by, for instance, five different concentrations for each alloying element. This means that in the case of a BMG with seven alloying elements, this 'optimization' would require determining properties of  $5^7 = 78\,125$  BMGs each having a different chemical composition. This is obviously unrealistic and should be replaced by a more economical mathematical optimization in order to reduce the number of BMG alloy candidates by orders of magnitude.

In order to reduce the number of experimentally evaluated alloys significantly, there has been a strong effort to develop and use several very complex mathematical models that are based on non-equilibrium thermodynamics of solids, thus minimizing the need for manufacturing and experimental evaluation of the actual alloy samples. However, the exclusive use of this strictly computational approach based on artificial neural networks (ANNs) alone [14] has been shown to have its own limitations concerning reliability and versatility as frankly demonstrated by Bhadeshia and Sourmail [15]. This is because ANNs are efficient and relatively accurate interpolating ('data mining') algorithms for multi-parameter functions, but they are not efficient and accurate search algorithms and they are definitely not reliable extrapolation algorithms. That is, the use of ANNs alone is not reliable for an 'out of the box' search outside of an initial experimental data set and therefore cannot be used for designing truly new BMGs with possibly significantly better multiple properties than any of the BMGs that might belong in the initial data set. Moreover, ANN requires a relatively large number of BMGs having different chemical concentrations to be manufactured and tested in order to provide a sufficiently reliable training set. Recently, an interesting effort using evolutionary optimization based on genetic algorithms [16] was made for designing new general purpose alloys, but the number of alloys that needed to be manufactured and experimentally evaluated for this approach is still too high.

Therefore, it is important to understand a need for mathematically sound multi-objective optimization algorithms [17] capable of confidently searching outside a given initial database and finding multiple options for the optimal chemical concentrations. However, the objective of this paper is not to educate classical materials scientists about the fine points of multi-objective evolutionary optimization algorithms, rather to provide a brief description of their main features and to demonstrate to readers the power and proven potential of using these advanced computational tools in designing new generations of alloys.

## 2. Multi-objective optimization algorithm

We propose a novel methodology for predicting the concentration of each of the important alloying elements in BMGs so that the new BMGs will have improved GFA and thermal stability. Specifically, we are currently concentrating on simultaneously maximizing  $T_g$ ,  $T_1$  and  $T_g/T_1$  and minimizing density of Zr-based BMGs [18, 19]. The proposed optimization

method is based on combining experimentally obtained multiple properties of the BMGs and a computational optimization algorithm [20–24] rather than on traditional experimentation alone, expert experience and intuition.

Specifically, the proposed BMG design method combines an advanced stochastic multi-objective evolutionary optimization algorithm based on self-organizing graph theory and a self-adapting response surface methodology [22, 25]. During the iterative computational design procedure, a small set of new BMG alloys is periodically predicted, manufactured and experimentally evaluated for their properties in order to continuously verify the accuracy of the entire design methodology [20–24]. The proposed BMG alloy design optimization method is thus experimentally verified. It minimizes the need for costly and time-consuming experimental evaluations of new BMG alloys and is capable of exploring BMG concentrations that are outside the initial data set thus providing a more economical and robust design tool than when using ANN or GA algorithms alone.

Specifically, the *multi*-objective optimization problem [17] maximizes not one objective function ( $T_{liq}$ ,  $T_g$ , etc) of design variables (chemical concentrations of each of the alloying elements in a given BMG), but simultaneously a number of often conflicting objectives (maximizing  $T_g$ ,  $T_l$  and  $T_g/T_l$ , while minimizing density). These objectives thus form a vector  $F(X)$  of  $n$  objective functions. The goal is to maximize this vector by simultaneously maximizing each of its components, that is,

$$\max F_i(\bar{X}) \quad \text{for } i = 1, \dots, n \quad (5)$$

subject to a vector of inequality constraints

$$g_j(\bar{X}) \leq 0 \quad \text{for } j = 1, \dots, m \quad (6)$$

and a vector of equality constraints

$$h_q(\bar{X}) = 0 \quad \text{for } q = 1, \dots, k. \quad (7)$$

The result of such a multi-objective optimization process is, in general, not unique. In the case of BMGs, this means that there will be possibly more than one alloy concentration that will satisfy the imposed constraints while having each of the optimized properties above their respective desired threshold values. These optimized BMG concentrations are said to form a Pareto front [17] composed of the ‘efficient non-dominated’ solutions, that is, the BMG concentrations for which it is not possible to improve any individual objective without deteriorating the values of at least some of the remaining objectives.

Classical gradient-based optimization algorithms [26, 27] are capable, under strict continuity and derivability hypotheses, of finding the optimal value only in the case of a single objective.. Unfortunately, such problems, as a rule, are difficult to formalize at the initial stage, since the user does not know initially what values of some objectives could be reached and how the remaining objectives will vary. That is, the user has very little if any *a priori* knowledge of objective functions’ space topology which is, in most cases, non-smooth. Furthermore, this approach is computationally very intensive and fails in situations where the Pareto front has discontinuities.

The least imaginative approach to BMG design could be to perform a general multi-objective optimization of the material properties. This strategy is the most accurate, but it requires an extremely large number of BMGs to be manufactured and tested in order to create an acceptably large data set. A hybrid multi-objective optimization concept [28] can accelerate the convergence to the Pareto front, but its main benefit is robustness, not speed, of the entire iterative approach to the Pareto front.

Another approach could involve formulation of a single optimization objective that may be the convolution of individual objectives with different weight coefficients assigned to each

of them thus creating a utility function [29]. However, the result of this strategy is only a single point on the Pareto front of optimal solutions (BMG concentrations). To obtain other points on the Pareto front, this entire optimization process would have to be repeated by choosing different sets of weight coefficients for the individual objective functions. Therefore, this approach was not used in this work. Instead, we used a true multi-objective optimization approach where each of the three objectives was extremized simultaneously [17] without any preferential weights among the objectives.

When performing multi-objective optimizations involving many simultaneous and often conflicting objectives and many design variables (e.g. concentrations of each of the alloying elements) and where each objective function evaluation (e.g. BMG alloy manufacturing and experimental evaluation of its multiple properties) is very costly, the only practical method of reducing the overall computing effort is to use metamodels or lower fidelity models. The most popular such method is to perform analytical fits of the available high fidelity (experimental) data to create multi-dimensional response surfaces (hyper-surfaces) [30]. Conceptually, this represents a multi-dimensional extension of the ‘one-dimensional curve fitting’ method or an extension of the well-known ‘one-parameter look-up tables’ method used by scientists and engineers in the past. Each of the objectives requires the creation of such a response surface and the dimensionality of each such response surface equals the number of the design variables (alloying elements in a BMG alloy).

Thus, in order to develop and realize the most effective optimization strategies, we have to perform a thorough preliminary search for the classes of base functions that will be able to construct the most accurate response surface models requiring the minimum number of high fidelity data (experimental data for BMGs each having different chemical concentrations). However, the number of experiments that is necessary for true multi-objective optimization problem solutions depends not only on the dimensionality of the problem (the number of alloying chemical elements in a BMG). It also depends, to a considerable degree, on the topologies of the objective functions. This is why any predictions concerning the necessary number of trial points (different BMG alloy concentrations) in the initial plan of experiment have a rather relative nature.

### *2.1. Conceptual features of IOSO optimization algorithm*

Because of its proven robustness, computing speed and versatility we have decided to use the multi-objective constrained indirect optimization based upon self-organization (IOSO) algorithm [18–24, 25]. This multi-objective optimization algorithm allows for concentrations of the alloying elements to be optimized so that several of the BMG alloy properties (maximizing  $T_g$ ,  $T_1$  and  $T_g/T_1$  and minimizing density) are simultaneously extremized, while satisfying a number of equality and inequality constraints (minimum and maximum specified concentrations for each of the alloying elements).

IOSO is a semi-stochastic multi-objective optimization algorithm incorporating certain aspects of a selective search on a continuously updated multi-dimensional response surface [18–25, 30]. Evaluations of objective functions ( $T_g$ ,  $T_1$ ,  $T_g/T_1$  and density) in this particular project were obtained utilizing experimental testing and verification of the BMG samples in order to determine optimum concentrations of each of the alloying elements.

The main benefits of the IOSO algorithm are its outstanding reliability in avoiding local minimums, its computational speed and a significantly reduced number of BMGs that need to be manufactured and experimentally evaluated as compared with more traditional gradient-based and genetic optimization algorithms. Also, the self-adapting multi-dimensional response surface formulation used by IOSO allows for the incorporation of realistic non-smooth



variations of experimentally obtained data and allows for accurate interpolation of such data using an efficient and accurate modified ANN algorithm.

Each iteration of the IOSO algorithm consists of two steps. The first step is the creation of approximations of the objective functions. Each iteration in this step represents a decomposition of the initial approximation functions into sets of simple approximation functions so that the final response surface functions are multi-level graphs. The second step is the optimization of coefficients in these approximation functions in order to fit the response surface as accurately as possible through the available high fidelity (experimental) data points.

To further minimize the computing time, during each iteration of IOSO, the optimization of the response surface function is performed only within the current search area. This step is followed by a direct call to an actual experimental evaluation for the obtained BMG concentration. During the IOSO operation, the information concerning the behavior of the objective function in the vicinity of the extremum is stored, and the response surface function is made more accurate only for this search area. While proceeding from one iteration to the next, the following steps are carried out: modification of the experiment plan, adaptive selection of current extremum search area, choice of the response surface function type (global or middle-range), transformation of the response surface function, modification of both parameters and structure of the optimization algorithms and, if necessary, selection of new promising points (optimized BMG concentrations). Thus, during each IOSO iteration, a series of response surface approximation functions for a particular objective of optimization is built. These functions differ from each other according to both structure and definition range. The subsequent optimization of these approximation functions, while accounting for uncertainties, allows us to determine a set of vectors of optimized variables (concentrations of alloying elements in the optimized BMGs). This approach allows for corrective updates of the structure and the parameters of the response surface approximation for each of the objective functions.

The distinctive feature of this multi-objective design optimization approach is a low number of trial points (BMGs that need to be manufactured and experimentally tested) to initialize the algorithm and that need to be created subsequently during each iteration with the IOSO optimization algorithm.

## 2.2. Proof-of-concept BMG design optimization results

The algorithms and approaches that we propose have a universal nature and are applicable to any complex engineering system. An example of our recently published application of IOSO optimization to design of Ni-based steel superalloys [20–24] is depicted in figure 3. It demonstrates the ability of the proposed methodology to immediately, in the first iteration, create the superalloys with properties that are superior to any of the alloys in the original experimental data set.

Our recent publications [18, 19] represent preliminary attempts to create a new generation of BMGs with improved multiple properties. Because of the unavailability of a large experimental data set for BMGs manufactured in a consistent manner, for the purpose of this study, we have decided to create such an experimental data set by combining data from several tables in the publications of Yi Li [31, 32]. Densities of all BMGs were computed by summing the products of concentrations of the alloying elements and their respective densities (at room temperature) given in table 1.

Those BMGs for which experimental data were incomplete or inconsistent in these publications were not taken into account. The final version of the initial population of experimentally evaluated BMGs had 53 alloys (table 2). In this work, we required that

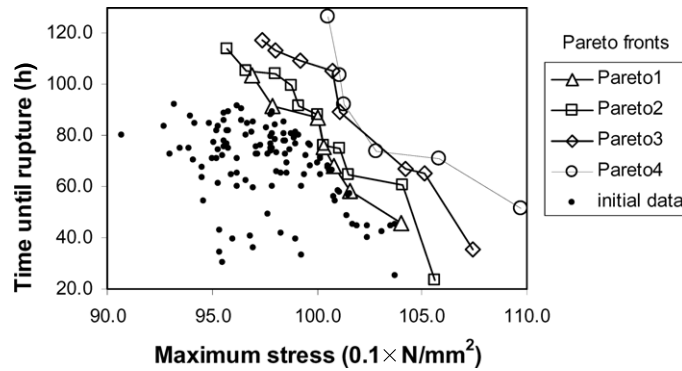


**Figure 3.** Experimental confirmation of the maximum stress at 20 °C and time-to-rupture at 975 °C for the initial data set of 120 Ni-base steel superalloys (black dots) and four generations of 20 Pareto-optimized Ni-base steel superalloys (other symbols) [21–24].

**Table 1.** Densities of the seven alloying elements used as design variables in the BMG optimization.

Element	Zr	Cu	Al	La	Cu,Ni	Pd	Si
Density ( $\text{g cm}^{-3}$ )	6.52	8.96	2.70	6.162	8.908	12.023	2.33

concentrations of all seven alloying ingredients (Zr, Cu, Al, La, (Cu,Ni), Pd, Si) should be used simultaneously as design variables. However, it should be noted that these 53 BMGs were not produced at the same time and that different sets of the BMGs were using only 3 alloying elements instead of all 7 alloying elements. Having such a disparate and incomplete initial data set of the available BMGs is making any interpolation, data mining, neural networks or optimization an extremely challenging task. It would have been much more advantageous to design an initial data set of BMGs by utilizing Sobol's algorithm [33] that would prescribe the semi-random chemical concentrations of these initial BMGs. The use of Sobol's algorithm is very helpful in distributing the initial concentrations in the best possible way so that the consequent multi-dimensional response surface fitting will be maximally accurate with the minimum number of experimentally evaluated BMGs. We did not have the luxury of manufacturing and experimentally evaluating the initial data set. This is why we had to use any published experimentally obtained data on the same class of BMGs that were manufactured and tested in the same laboratory, thus, presumably under same conditions.

We then specified that new Pareto-optimal BMGs be created by the IOSO algorithm while simultaneously maximizing  $T_g$  and  $T_l$  or while simultaneously maximizing  $T_g$  and  $T_{rg}$ . The third simultaneous objective, minimizing the density of the new BMGs, was also implemented.

Initial data from table 2 were used as an input to IOSO optimization algorithm with a request that it creates 50 new BMGs that should belong to a Pareto-optimal front when simultaneously maximizing  $T_g$  and  $T_l$  without minimizing new BMG densities. Optimization results after one iteration cycle with IOSO are shown in table 3 and in figures 4 and 5.

Table 3 shows the optimized concentrations [18, 19] of each of the 7 alloying elements and the corresponding maximized values of  $T_g$  and  $T_l$  for the resulting 50 Pareto-optimal BMGs. Note that  $T_{rg}$  values and densities of these optimized BMGs are also shown in table 3, although the goal of this two-objective optimization problem was not to explicitly maximize  $T_{rg}$  values or minimize densities of the new BMGs.

A more realistic BMG optimization test case was then created that represented an example of a three-objective optimization that involved simultaneously maximizing  $T_g$  and  $T_{rg}$ , while



**Table 2.** Experimental data for 53 BMGs collected from published works of Yi Li [31, 32].

#	Zr (%)	Cu (%)	Al (%)	La (%)	Cu,Ni (%)	Pd (%)	Si (%)	$T_g$ (K)	$T_i$ (K)	$T_{rg} = T_g/T_i$	$\rho$ (g cm <sup>-3</sup> )
1	50	36	14	0	0	0	0	724	1188	0.609	6.8636
2	50	38	12	0	0	0	0	722	1170	0.617	6.9888
3	50	40	10	0	0	0	0	714	1176	0.607	7.1140
4	50	43	7	0	0	0	0	703	1181	0.595	7.3018
5	49	44	7	0	0	0	0	704	1184	0.594	7.3262
6	48	45	7	0	0	0	0	708	1186	0.596	7.3506
7	49	45	6	0	0	0	0	704	1187	0.593	7.3888
8	48	46	6	0	0	0	0	706	1192	0.592	7.4132
9	49	46	5	0	0	0	0	701	1195	0.586	7.4514
10	49	47	4	0	0	0	0	697	1208	0.576	7.5140
11	45	49	6	0	0	0	0	717	1178	0.608	7.4864
12	45	50	5	0	0	0	0	714	1185	0.602	7.5490
13	44	51	5	0	0	0	0	719	1189	0.604	7.5734
14	45	48	7	0	0	0	0	720	1188	0.606	7.4238
15	45	47	8	0	0	0	0	722	1195	0.604	7.3612
16	46	49	5	0	0	0	0	711	1193	0.595	7.5246
17	47	49	4	0	0	0	0	704	1204	0.584	7.5628
18	54	38	8	0	0	0	0	692	1190	0.581	7.1416
19	56	36	8	0	0	0	0	685	1212	0.565	7.0928
20	52	38	10	0	0	0	0	705	1163	0.606	7.0652
21	54	36	10	0	0	0	0	698	1176	0.593	7.0164
22	54	40	6	0	0	0	0	684	1216	0.562	7.2668
23	0	0	12.4	70	17.6	0	0	403	759	0.530	6.2160
24	0	0	13.2	68	18.8	0	0	407	742	0.548	6.2212
25	0	0	14	66	20	0	0	405	674	0.600	6.2265
26	0	0	14.6	64.6	20.8	0	0	414	696	0.594	6.2277
27	0	0	15.2	63.1	21.7	0	0	420	699	0.600	6.2316
28	0	0	15.7	62	22.3	0	0	422	722	0.584	6.2308
29	0	0	15.9	61.4	22.7	0	0	426	729	0.584	6.2348
30	0	0	16.3	60.5	23.2	0	0	423	727	0.581	6.2347
31	0	0	16.6	59.6	23.8	0	0	426	743	0.573	6.2408
32	0	0	17	58.6	24.4	0	0	431	764	0.564	6.2434
33	0	0	17.5	57.6	24.9	0	0	435	783	0.555	6.2399
34	0	0	17.9	56.5	25.6	0	0	440	813	0.541	6.2452
35	0	0	18.4	55.4	26.2	0	0	436	844	0.516	6.2444
36	0	0	20.5	50.2	29.3	0	0	435	930	0.467	6.2568
37	0	0	14	70	16	0	0	404	763	0.529	6.1166
38	0	0	14	68	18	0	0	405	724	0.559	6.1716
39	0	0	14	66	20	0	0	405	674	0.600	6.2265
40	0	0	14	64	22	0	0	411	715	0.574	6.2814
41	0	0	14	62	24	0	0	417	738	0.565	6.3363
42	0	0	14	59	27	0	0	422	773	0.545	6.4187
43	0	0	14	57	29	0	0	427	815	0.523	6.4736
44	0	2	0	0	0	81.5	16.5	633	1097.3	0.576	10.3624
45	0	4	0	0	0	79.5	16.5	635	1086.0	0.584	10.3011
46	0	6	0	0	0	77.5	16.5	637	1058.1	0.602	10.2398
47	0	8.2	0	0	0	75	16.8	645	1135.9	0.567	10.1434
48	0	10.2	0	0	0	73	16.8	652	1153.6	0.565	10.0821
49	0	36	14	50	0	0	0	428	862.7	0.496	6.6846
50	0	26	14	60	0	0	0	404	785.6	0.514	6.4048
51	0	20	14	66	0	0	0	395	731.0	0.540	6.2369
52	0	14	14	72	0	0	0	391	792.7	0.493	6.0690
53	0	10	14	76	0	0	0	361	825.5	0.437	5.9571

**Table 3.** Results of IOSO optimization when maximizing  $T_g$  and  $T_l$  without minimization of BMG density: concentrations of alloying elements,  $T_g$ ,  $T_l$ ,  $T_{rg}$  and density of the 50 Pareto-optimal BMGs predicted after the first iteration with IOSO using experimental data from table 2.

#	Zr (%)	Cu (%)	Al (%)	La (%)	Cu,Ni (%)	Pd (%)	Si (%)	$T_g$ (K)	$T_l$ (K)	$T_{rg} = T_g/T_l$	$\rho$ (g cm <sup>-3</sup> )
1	58.000	0.000	0.000	30.189	4.452	0.027	2.291	671.7	1243.3	0.540	6.0951
2	56.996	9.919	0.000	24.719	3.769	0.002	2.111	672.0	1242.7	0.540	6.5133
3	58.000	14.664	0.003	17.215	4.617	0.000	1.807	672.1	1242.4	0.540	6.6097
4	57.820	11.863	0.997	25.583	4.227	0.000	1.636	672.4	1241.8	0.541	6.8507
5	57.744	12.840	1.280	26.893	4.362	0.000	1.483	672.6	1241.3	0.541	7.0301
6	57.631	14.539	1.491	28.886	4.161	0.001	1.439	672.8	1240.7	0.542	7.2847
7	58.000	21.764	0.604	9.096	4.360	0.231	3.211	673.1	1240.2	0.542	6.7994
8	57.654	15.215	2.087	27.989	4.172	0.000	1.343	673.2	1239.7	0.543	7.3062
9	56.681	16.364	2.144	31.139	4.032	0.055	1.606	673.5	1239.0	0.543	7.5416
10	56.710	15.044	2.553	33.863	4.059	0.048	1.699	673.8	1238.4	0.544	7.6079
11	57.710	26.463	0.090	23.266	0.194	0.176	0.635	674.3	1238.0	0.544	7.6230
12	57.467	27.146	0.105	24.274	0.158	0.306	0.553	674.7	1237.2	0.545	7.7416
13	57.359	28.139	0.029	25.283	0.327	0.187	0.790	675.3	1236.1	0.546	7.8898
14	56.602	28.001	0.121	21.653	0.204	0.564	0.407	675.6	1235.5	0.546	7.6322
15	56.255	28.317	0.125	19.583	0.203	0.503	0.240	676.0	1234.8	0.547	7.4992
16	56.124	28.685	0.185	20.111	0.232	0.873	0.394	676.3	1234.1	0.548	7.6083
17	56.197	29.121	0.169	20.089	0.290	0.963	0.382	676.7	1233.6	0.548	7.6662
18	56.496	29.745	0.343	16.291	0.000	1.782	0.056	677.0	1232.9	0.549	7.5773
19	56.230	29.941	0.134	18.502	0.269	1.021	0.231	677.4	1232.3	0.549	7.6446
20	56.276	30.303	0.412	16.197	0.022	2.037	0.058	677.7	1231.7	0.550	7.6417
21	56.437	30.951	0.166	16.413	0.233	1.356	0.025	678.3	1230.8	0.551	7.6531
22	55.982	30.864	0.129	17.015	0.186	1.691	0.015	678.7	1230.3	0.551	7.6876
23	55.528	30.871	0.216	16.849	0.300	1.590	0.003	679.1	1229.5	0.552	7.6485
24	55.562	31.317	0.018	17.305	0.065	1.551	0.034	679.7	1228.6	0.553	7.6883
25	55.482	31.457	0.042	17.544	0.064	1.707	0.031	680.0	1228.1	0.553	7.7298
26	55.555	31.786	0.012	16.869	0.096	1.396	0.025	680.4	1227.5	0.554	7.6869
27	55.633	32.308	0.000	16.591	0.398	1.538	0.000	681.2	1226.4	0.555	7.7648
28	55.648	32.560	0.000	16.397	0.108	1.256	0.001	681.6	1225.8	0.556	7.7166
29	55.273	32.525	0.012	16.159	0.217	1.244	0.002	682.0	1225.1	0.556	7.6829
30	54.966	32.587	0.057	16.720	0.213	1.205	0.001	682.4	1224.4	0.557	7.6992
31	55.166	32.965	0.029	16.576	0.208	1.217	0.000	682.9	1223.7	0.558	7.7375
32	54.731	32.862	0.000	16.310	0.303	2.025	0.000	683.3	1223.1	0.558	7.7883
33	54.344	32.808	0.012	18.397	1.031	1.257	0.000	683.7	1222.5	0.559	7.8597
34	54.190	32.856	0.028	18.817	1.122	1.414	0.001	684.0	1222.0	0.559	7.9071
35	54.752	33.555	0.134	19.251	1.300	1.279	0.000	684.5	1221.3	0.560	8.0357
36	54.339	33.436	0.091	17.609	0.255	1.052	0.009	684.9	1220.7	0.561	7.7757
37	54.618	33.822	0.066	16.965	0.230	0.993	0.000	685.3	1220.2	0.561	7.7785
38	54.649	34.086	0.079	16.837	0.429	1.508	0.021	685.8	1219.5	0.562	7.8768
39	54.653	34.423	0.228	13.737	0.260	0.716	0.094	686.3	1218.6	0.563	7.6116
40	54.596	34.514	0.218	13.335	0.221	0.651	0.092	686.6	1218.2	0.563	7.5797
41	53.967	34.233	0.168	17.456	0.735	0.785	0.000	687.0	1217.7	0.564	7.8260
42	54.248	34.538	0.000	20.010	0.000	1.185	0.000	687.4	1217.2	0.564	8.0070
43	55.477	35.689	0.041	18.214	0.251	1.785	0.011	688.0	1216.6	0.565	8.1754
44	54.000	34.788	0.088	12.031	0.003	0.540	0.011	688.2	1216.1	0.565	7.4469
45	54.114	35.039	0.002	12.841	0.013	0.390	0.011	688.7	1215.5	0.566	7.5073
46	13.810	51.000	16.473	0.000	14.741	60.837	0.007	724.8	1215.5	0.596	14.5425
47	15.242	50.803	16.863	0.018	15.434	52.467	0.001	724.9	1215.0	0.596	13.6850
48	15.651	50.975	17.157	0.001	15.115	53.317	0.000	725.0	1214.5	0.596	13.8078
49	15.494	50.989	17.326	0.180	15.153	55.427	0.000	725.0	1214.2	0.597	14.0715
50	15.727	51.000	17.515	0.000	15.345	55.044	0.000	725.0	1213.7	0.597	14.0527

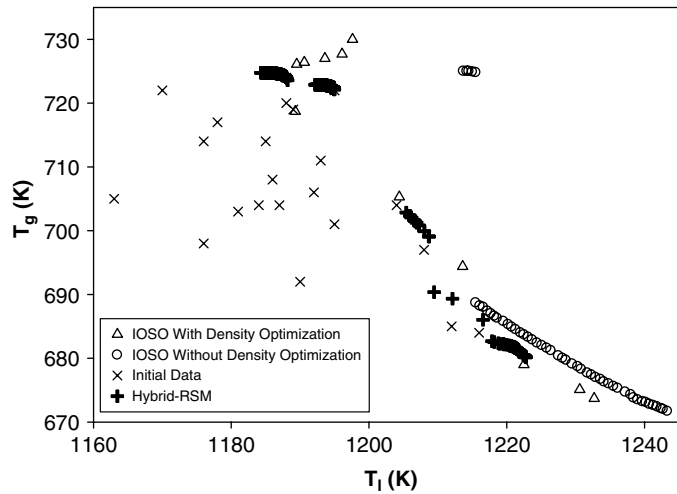


**Figure 4.** Best BMGs from the original data set given in table 2 (x x x x), discontinuous Pareto front of 50 optimized BMGs given in table 3 (o o o o) when simultaneously maximizing  $T_g$  and  $T_l$  without density minimization using IOSO software, Pareto front of optimized BMGs given in table 4 ( $\Delta \Delta \Delta \Delta$ ) when simultaneously maximizing  $T_g$  and  $T_l$  and minimizing density using IOSO software, discontinuous Pareto front of optimized BMGs (+++++) when simultaneously maximizing  $T_g$  and  $T_l$  and minimizing density using our hybrid multi-objective optimization and radial basis function based response surface software.

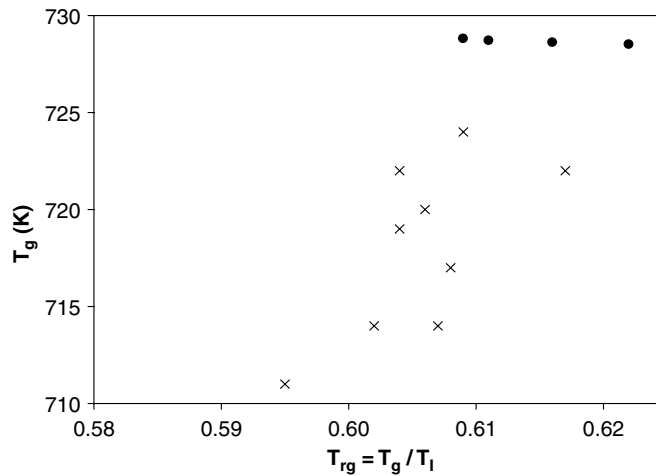


**Figure 5.** A set of best BMGs (x x x x) from the initial data set (table 2) and Pareto-optimized BMGs (•••••) given in table 5 when simultaneously maximizing  $T_g$  and  $T_{rg}$  without density minimization.

minimizing the density of BMGs. The IOSO optimizer was requested to create Pareto-optimal BMGs for this problem starting with the initial data set given in table 2. Optimization results of this three-objective optimization case after one iteration cycle with IOSO are shown in table 4. These results represent concentrations of each of the 7 alloying elements and simultaneously optimized values of  $T_g$ ,  $T_l$  and densities for the resulting 28 Pareto-optimal BMGs.  $T_{rg}$  values of these optimized BMGs are shown in table 4, although the goal of this three-objective optimization problem was not to explicitly maximize  $T_{rg}$  values of the new BMGs.

**Table 4.** Results of IOSO optimization when maximizing  $T_g$  and  $T_l$  while minimizing density of BMGs: optimized concentrations of alloying elements,  $T_g$ ,  $T_l$ ,  $T_{rg}$  and density of Pareto-optimal BMGs predicted after the first iteration with IOSO using experimental data from table 2.

No.	Zr (%)	Cu (%)	Al (%)	La (%)	Cu,Ni (%)	Pd (%)	Si (%)	$T_g$ (K)	$T_l$ (K)	$T_{rg} = T_g/T_l$	$\rho$ (g cm <sup>-3</sup> )
1	57.999	30.770	0.002	0.001	0.000	0.001	11.227	673.5	1232.7	0.547	6.799
2	53.330	29.935	0.770	0.000	0.000	0.000	15.964	675.1	1230.7	0.548	6.552
3	56.866	38.133	4.974	0.000	0.000	0.000	0.022	679.1	1222.5	0.556	7.260
4	50.227	47.223	1.060	0.000	0.000	0.000	1.489	694.3	1213.3	0.571	7.569
5	39.138	46.942	2.272	0.000	0.001	0.001	11.645	705.5	1204.7	0.586	7.090
6	32.645	50.993	11.075	0.001	0.000	0.001	5.282	730.1	1197.5	0.608	7.119
7	38.960	50.384	9.723	0.000	0.000	0.000	0.931	727.7	1196.3	0.608	7.335
8	48.256	34.613	16.486	0.000	0.000	0.000	0.643	727.0	1193.4	0.609	6.705
9	40.999	43.022	15.859	0.001	0.000	0.001	0.117	726.4	1190.3	0.610	6.955
10	37.970	41.550	15.124	0.001	0.000	0.000	5.344	726.1	1189.2	0.610	6.730
11	44.287	50.864	4.847	0.000	0.000	0.000	0.000	718.7	1189.0	0.603	7.577
12	0.393	17.233	0.216	0.064	0.000	73.758	8.334	653.5	1157.1	0.565	10.640
13	0.001	0.000	1.053	2.568	0.008	81.017	15.353	632.1	1095.4	0.575	10.285
14	0.500	0.134	0.223	9.268	0.024	81.111	8.731	631.6	1093.0	0.576	10.582
15	3.368	0.546	1.437	12.258	0.036	81.500	0.853	631.3	1091.5	0.578	10.888
16	0.005	8.134	6.062	4.713	0.321	70.319	10.449	638.5	1060.1	0.601	9.905
17	0.006	5.965	0.008	0.000	0.000	77.330	16.689	637.1	1058.8	0.601	10.215
18	0.000	0.032	19.880	45.000	29.282	0.000	5.805	434.9	934.5	0.467	6.055
19	0.000	1.449	20.497	41.613	26.367	0.000	10.074	435.1	920.3	0.471	5.830
20	0.000	36.014	13.996	49.973	0.002	0.000	0.008	428.0	862.5	0.495	6.684
21	0.000	0.001	16.255	50.100	28.670	0.000	4.971	432.9	830.5	0.526	6.197
22	0.000	25.735	15.300	42.810	2.378	0.000	13.770	417.1	827.1	0.503	5.888
23	0.000	0.001	13.918	56.909	29.090	0.000	0.080	427.0	815.8	0.524	6.478
24	0.000	9.318	16.130	63.464	0.000	0.000	11.087	389.5	796.5	0.488	5.438
25	0.000	26.620	13.917	59.456	0.000	0.000	0.000	404.8	789.1	0.514	6.426
26	0.000	0.0137	12.416	70.057	17.513	0.000	0.001	402.9	759.3	0.531	6.216
27	0.000	0.001	19.297	59.590	20.460	0.000	0.651	426.4	739.3	0.577	6.032
28	0.000	5.422	18.150	50.853	17.858	0.000	7.717	423.0	724.7	0.584	5.881

In order to confirm the reliability of the IOSO optimization software for design of these types of alloys, we also used our own hybrid multi-objective optimization algorithm [34] coupled with our response surface generation scheme based on polynomials of radial basis functions [30, 35]. It is remarkable that although these two multi-objective optimization algorithms use vastly different concepts, their results (see figure 4) are in good agreement despite the fact that the initial data set is very small (only 53 alloys) and that it is only loosely connected since none of the initial BMGs has more than three alloying elements.

In order to gain some understanding of the behavior of other objectives when one of the most important GFA parameters,  $T_{rg}$ , is maximized, we repeated the entire optimization process by requesting that the IOSO algorithm generate concentrations of the alloying elements for Pareto optimal BMGs that will simultaneously maximize  $T_g$  and  $T_{rg}$  without minimizing density of the BMGs. The results are given in table 5 and also depicted in figure 5. It is evident that the optimization process resulted in a new generation of BMGs with superior values of  $T_{rg}$ .

In figure 6, it is educative to see the comparison of  $T_g$  and  $T_{rg}$  values plotted against the densities of the BMGs for all four cases: initial data set of 53 BMGs, two-objective optimized set of 50 BMGs when the density of each alloy was not explicitly minimized, three-objective optimized set of 28 BMGs when the density was minimized simultaneously as  $T_g$  and  $T_l$  were maximized and the 4 BMGs obtained in the two-objective case when  $T_g$  and  $T_{rg}$  were maximized without explicitly minimizing the density.

**Table 5.** Results of optimization when simultaneously maximizing  $T_g$  and  $T_{rg}$  without minimizing density of BMGs: concentrations of alloying elements,  $T_g$ ,  $T_{liq}$ ,  $T_{rg}$  and density of four best Pareto-optimal BMGs predicted after the first iteration with IOSO using experimental data from table 2.

No.	Zr (%)	Cu (%)	Al (%)	La (%)	(Cu,Ni) (%)	Pd (%)	Si (%)	$T_g$ (K)	$T_l$ (K)	$T_{rg} = T_g / T_l$	$\rho$ (g cm <sup>-3</sup> )
1	40.585	31.857	20.479	0.000	0.000	0.001	7.078	728.8	1196.1	0.609	6.21
2	36.500	41.391	16.168	0.000	0.000	0.001	5.943	728.7	1193.3	0.611	6.65
3	35.532	41.048	16.024	0.000	0.000	0.001	7.397	728.6	1182.6	0.615	6.60
4	45.883	37.665	4.770	0.000	0.000	0.002	11.685	728.5	1170.5	0.621	6.78

It is evident that the Pareto front is not continuous in some of these cases. Notice that in such situations, the optimization approach that uses a linear combination of weighted individual objectives and forms a single utility function would not perform well if the choice of the weight factors is such that creates a search direction which passes through a gap in the Pareto front.

A three-dimensional perception of the relationship between alloy density,  $T_g$ , and  $T_l$  (figure 7) should help in understanding that the initial data set (table 2) was highly disconnected. Also, the initial data set was quite small, while the optimization task was very ambitious (optimize concentrations of 7 alloying elements for two or three simultaneous objectives by creating a Pareto front having optimized BMGs).

Each of the initial BMGs had only three alloying elements instead of the 7 alloying elements that were allowed to serve as design variables. To create seven-dimensional response surfaces using such an incomplete and small initial data set was a challenge. Nevertheless, the IOSO optimization algorithm with its self-adaptive response surface methodology was able to work with such incomplete data and produce better results in just one iteration. From all of these figures it is evident that the Pareto-optimized BMGs have better multiple properties than those BMGs that belong to the initial data set of BMGs.

### 3. Inverse design of BMGs for specified performance

An inverse design option [23, 36] of this computational methodology has also been developed. It has the capability of designing a number of BMG alloys with the same multiple properties, but having different concentrations of the alloying elements. This will make their availability, cost and utility more affordable. Specifically, we utilized [18, 19] the original experimental data set (table 2) and IOSO optimization algorithm to determine chemical concentrations of the seven alloying elements (Zr, Cu, Al, La, (Cu,Ni), Pd, Si) in a number of new BMGs that will all have  $T_g = 680$  K for different values of  $T_l$  (1000 K, 1100 K, 1200 K, 1240 K). Results of such inverse design optimization of BMGs are depicted in figure 8. These results confirm intuitive expectations that with the increase in  $T_l$ , the inversely designed BMGs should have higher concentrations of Zr and La, while having lower concentrations of Pd, Al, and Si.

### 4. Summary of the proposed BMG design optimization methodology

Based on the literature survey [1–13], Zr, Ti, Cu, Ni, Mg, Al, Fe, Nb, Si and Sn have been the most commonly used elements and should be considered for this type of computational optimization and experimental testing to achieve the best BMG compositions. However, a number of other alloying elements could be utilized if they satisfy the basic glass forming abilities suggested by Inoue and listed in the introductory part of this paper.

In our design optimization methodology presented here, it is necessary that the user specifies the minimum and the maximum expected concentrations of a finite number of the

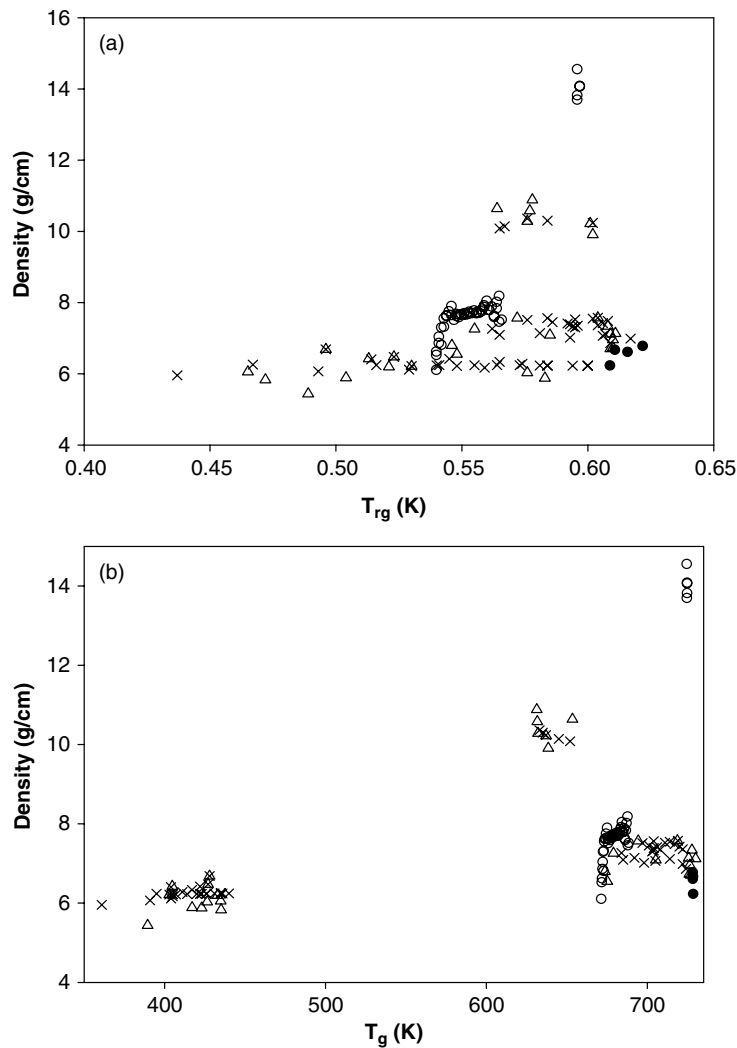


**Figure 6.** Comparison of optimization results when simultaneously optimizing  $T_g$  and  $T_l$ : (a) values of  $T_{rg}$  versus density of the BMGs; (b) values of  $T_g$  versus density of the BMGs. Here, ( $\times \times \times$ ) represents initial data set of BMGs (table 2), ( $o o o o$ ) depicts Pareto-optimized BMGs without density minimization (table 3), ( $\Delta \Delta \Delta \Delta$ ) are Pareto optimized BMGs when also minimizing density of each new BMG (table 4), while ( $\bullet \bullet \bullet \bullet$ ) depicts Pareto optimized BMGs when maximizing  $T_g$  and  $T_{rg}$  without density minimization (table 5).

most important BMG alloying elements. If the number of such elements is approximately five or six and the number of simultaneous objectives is two or three, from our experience with optimizing Ni-base superalloys [20–24], we expect that an initial database of approximately 80 BMGs has to be developed. These 80 initial BMGs then must be manufactured by casting them in an identical manner, thus avoiding variability in the manufacturing process. These casts should be then experimentally tested for the specified number of simultaneous objectives.

This information is then used for building approximation functions (multi-dimensional response surfaces) which will further be enriched by the optimization algorithm using modified radial basis functions and multiple ANNs. These approximation functions are then optimized



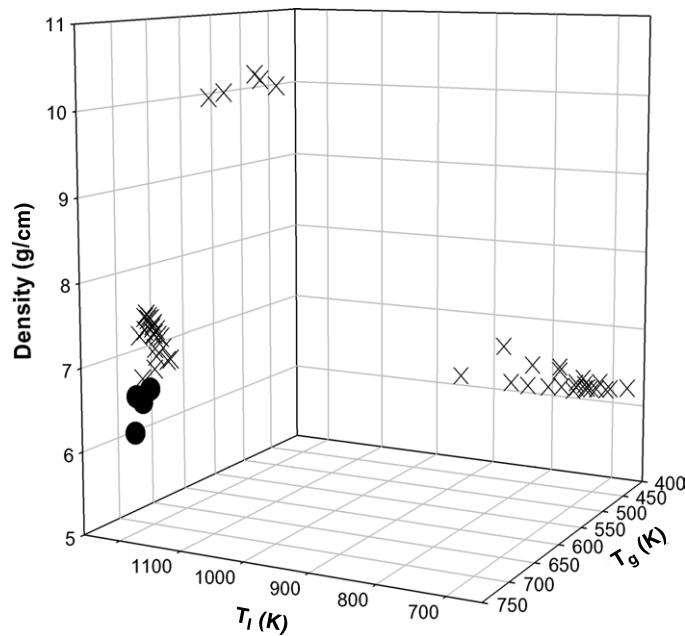


**Figure 7.** A three-dimensional perspective view of the density  $T_g - T_i$  space depicting widely scattered property values for the initial data set of BMGs from table 2 ( $\times \times \times \times$ ) and a compact set of BMGs from table 5 ( $\bullet \bullet \bullet \bullet$ ) when simultaneously maximizing  $T_g$  and  $T_{rg}$  without minimizing density.

using a non-gradient-based, robust, multi-objective optimization algorithm [17, 25, 28, 34]. At each optimization iteration, a multi-criterion optimization task with a specified number of Pareto front optimal points (most likely 10) needs to be solved. The results of this complex numerical optimization process will be chemical concentrations of 5–6 specified alloying elements in these 10 new BMGs which the optimization algorithm predicted as belonging to the non-dominated Pareto-optimal front, while accounting for a specified level of uncertainty of BMG casting and testing.

Since the multi-dimensional response surfaces are fitted using a large number of points created by the ANNs and the radial basis functions, instead of exclusively experimental data, the initial accuracy of the fit of the response surface will be relatively low. Consequently, it could be expected that not all of the 10 new optimized BMGs are actually superior to all of the initial 80 BMGs. To clarify this point, these 10 optimized BMGs then need to be manufactured and experimentally evaluated for the multiple properties. This concludes the first design iteration. The second iteration starts by using all ( $80 + 10 = 90$ ) experimentally evaluated BMGs. The response surface building, enrichment and optimization process is then repeated using these 90 data points with the same multiple objectives. The 10 newly Pareto-optimized BMGs then need to be manufactured and experimentally tested to confirm that most of them are better than any of the 90 BMGs used in the second iteration of the design optimization process. The third iteration then starts with all accumulated experimentally tested BMGs ( $80 + 10 + 10 = 100$ ), repeats all optimization steps and results in 10 new optimized BMGs. The entire iterative process continues typically 4–5 cycles until the Pareto front sufficiently converges.

It should be pointed out that evolutionary optimization algorithms do not automatically provide sensitivities of the objective functions with respect to each design variable (alloying

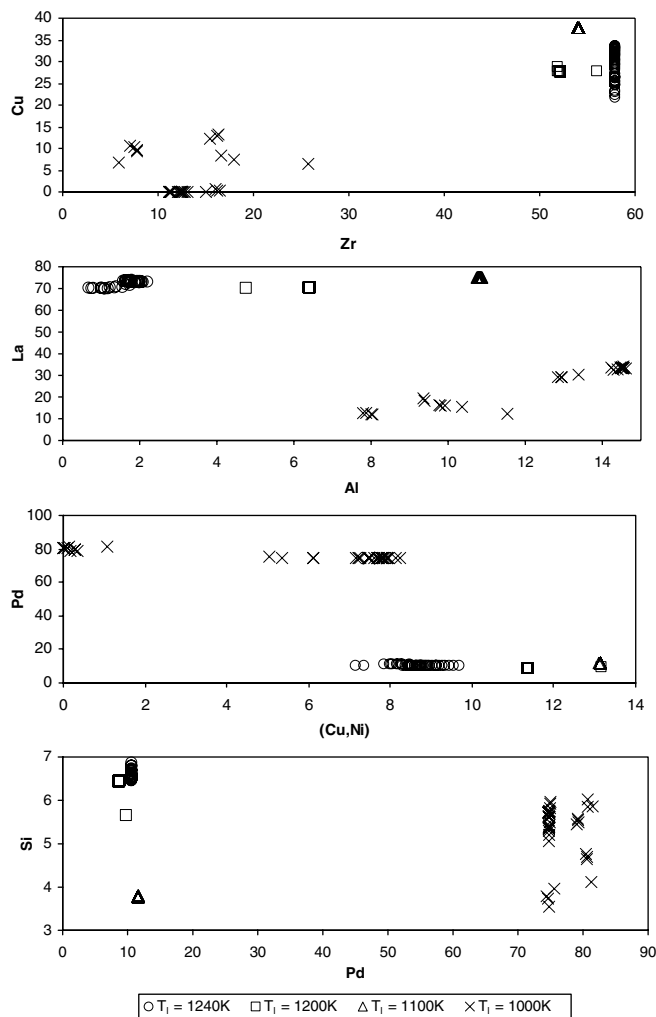


**Figure 8.** Results of an inverse design optimization problem:  $T_g = 680$  K,  $T_1 =$  variable [19]. Example showing inversely determined concentrations of alloying elements for these conditions.

element variation of concentration). This is because the evolutionary based optimizers do not employ gradients of the objective functions when performing a search for the optima. However, not all of the alloying elements in an alloy contribute significantly towards the Pareto objectives in questions. Such sensitivity analysis could be performed in an *a posteriori* fashion after the evolutionary optimization is completed by using, for example, finite differencing [37] of perturbed Pareto-optimal solutions. Recently, a methodology has been suggested [38] where, for example, out of a total of 108 variables, just one was actually found to influence the objectives in question! This is remarkable and suggests that the alloy design using the traditional cut-and-try approach of including and keeping those alloying elements that seem to be influential in a similar type of alloys often leads to unnecessarily expensive and complex new alloys.

However, this should not preclude future alloy designers from using initially a large number of alloying elements in the optimization process, because evaluation of the multiple properties

of the new alloys does not have to be performed with classical experimental techniques. Specifically, there are several commercially available software packages such as JMatPro [39] and FactSage [40] that allow users to specify concentrations of each of the alloying elements and predict multiple properties of such virtual alloys quickly, cheaply and with a high degree of precision [41].

Regretfully, despite decades of non-equilibrium thermodynamics theoretical deliberations, mostly anecdotal visual observations of the microstructure and exhaustive trial-and-error experimentation, the improvements in the GFA of the known BMG alloys have been incremental at best. As a consequence, none of the commercially available software used for the design of alloys has successfully ventured in the field of BMG design. Even atomistic modeling (*ab initio* modeling) based on purely theoretical approaches to the design of BMGs has run into serious difficulties when having more than three alloying elements in a BMG. Consequently, at the present time, a combination of robust multi-objective optimization algorithms and experimentally obtained multiple properties of BMGs appears to be a viable option for design of new generations of improved BMGs. It should be emphasized that this is a design method, not an analysis method. Thus, its goal is to efficiently design improved generations of alloys, not to analyze the existing alloys and speculate about the insights of the how and why of glass formation.

## 5. Conclusions

A new method was demonstrated that offers a realistic possibility of predicting chemical concentrations of a number of new BMG alloys so that the new alloys will have superior properties. The new BMG design concept uses a combination of a multi-objective stochastic optimization algorithm and experimental data for thermo-mechanical properties while requiring a minimum number of experimental evaluations of the candidate BMGs, in order to verify the computational results. Conceptually, this design approach could include additional objectives such as minimized cooling speed, maximized  $T_{\text{rg}}$ , maximized hardness, maximized modulus of elasticity and minimized cost of raw materials.

## Acknowledgments

The authors are grateful for the partial financial support provided for this work by the United States Army Research Office under the grant 50486-MS-H monitored by Dr William M Mullins and by a research grant FA9550-06-1-0170 from the Air Force Office of Scientific Research monitored by Dr Todd E Combs, Dr Fariba Fahroo and Dr Donald Hearn. The authors are also grateful for the copies of pertinent publications kindly provided by Professor Yi Li of the National University of Singapore and for the invaluable advice provided by Dr Laszlo Kecskes of Army Research Laboratory at Aberdeen Proving Grounds, Maryland, and Professor Todd Hufnagel of The Johns Hopkins University. Final graphical work was performed by Mr Carlos Velez of the MAIDROC Laboratory at the Florida International University.

## References

- [1] Johnson W L 1999 Bulk glass-forming metallic alloys: science and technology *MRS Bull.* **24** 45–56
- [2] Klement W, Willens R H and Duwez P 1960 Non-crystalline structure in solidified gold–silicon alloys *Nature (London)* **187** 869–70
- [3] Drehman J, Greer A L and Turnbull D 1982 Bulk formation of metallic glass: Pd<sub>40</sub>Ni<sub>40</sub>P<sub>20</sub> *Appl. Phys. Lett.* **41** 716–7
- [4] Inoue A 2000 Stabilisation of metallic supercooled liquid and bulk amorphous alloys *Acta Mater.* **48** 279–306

- [5] Inoue A and Takeuchi A 2004 Recent progress in bulk glassy, nanoquasicrystalline and nanocrystalline alloys *Mater. Sci. Eng. A* **375–377** 16–30
- [6] Fan G J, Choo H and Liaw P K 2007 A new criterion for the glass-forming ability of liquids *J. Non-Cryst. Solids* **353** 102–7
- [7] Lu Z P and Liu C T 2002 A new glass-forming ability criterion for bulk metallic glasses *Acta Mater.* **50** 3501–12
- [8] Kecskes L J, Trevino S F and Woodman R H 2002 Glass-forming ability and crystallization behavior in high-density bulk metallic glasses *Proc. 2002 MRS Symp. (MRS, Warrendale, PA)* vol 754 pp 377–84
- [9] Zhang Y, Zhao D Q, Pan M X and Wang W H 2003 Glass forming properties of Zr-based bulk metallic alloys *J. Non-Cryst. Solids* **315** 206–10
- [10] Xu D, Lohwongwatana B, Duan G, Johnson W L and Garland C 2004 Bulk metallic glass formation in binary Cu-rich alloy series  $\text{-Cu}_{100-x}\text{Zr}_x$  ( $x = 34.36, 38.2, 40\%$ ) and mechanical properties of bulk  $\text{Cu}_{64}\text{Zr}_{36}$  glass *Acta Mater.* **52** 2621–4
- [11] Stoica M, Eckert J, Roth S and Schultz L 2004 Preparation of bulk amorphous Fe–Cr–Mo–Ga–P–C–B alloys by copper mold casting *Mater. Sci. Eng. A* **375–377** 399–402
- [12] Na J H, Kim W T, Kim D H and Yi S 2004 Bulk metallic glass formation in Ni–Zr–Nb–Al alloy systems *Mater. Lett.* **58** 778–82
- [13] Zhang Q S, Zhang H F, Deng Y F, Ding B Z and Hu Z Q 2003 Bulk metallic glass formation of Cu–Zr–Ti–Sn alloys *Scr. Mater.* **49** 273–8
- [14] Bhadeshia H K D H 1999 Neural networks in materials science *ISIJ Int.* **39** 966–79
- [15] Bhadeshia H K D H and Sourmail T 2003 Design of creep-resistant steels: success and failure of models *Japan Soc. Promotion of Science, 123rd Committee on Heat-Resisting Materials and Alloys (Tokyo, Japan)* vol 44 pp 299–314
- [16] Chakraborti N 2004 Genetic algorithms in materials design and processing *Int. Mater. Rev.* **49** 246–60
- [17] Deb K 2002 *Multi-Objective Optimization Using Evolutionary Algorithms* (New York: Wiley)
- [18] Dulikravich G S and Egorov I N 2006 Optimizing chemistry of bulk metallic glasses for improved thermal stability *Symp. on Bulk Metallic Glasses: TMS 2006 Annual Meeting Exhibition (San Antonio, TX, 12–16 March 2006)* ed P K Liaw and R A Buchanan
- [19] Dulikravich G S, Egorov I N and Jelisavcic N 2006 Evolutionary optimization of chemistry of bulk metallic glasses *Proc. III European Conf. on Computational Solid and Structural Mechanics (Lisbon, Portugal, 5–8 June 2006)* ed C A Mota Soares *et al* (Heidelberg: Springer)
- [20] Dulikravich G S, Egorov I N, Sikka V K and Muralidharan G 2003 Semi-stochastic optimization of chemical composition of high-temperature austenitic steels for desired mechanical properties *2003 TMS Annual Meeting, Yazawa Int. Symp.: Processing and Technologies (San Diego, CA, 2–6 March 2003)* vol 1 ed F Kongoli *et al* (Warrendale, PA: Minerals, Metals and Materials Society) pp 801–14
- [21] Yegorov-Egorov I N and Dulikravich G S 2004 Optimization of alloy chemistry for maximum stress and time-to-rupture at high temperature *10th AIAA/ISSMO Multidisciplinary Analysis and Optimization Conf. (AIAA, Albany, NY, 30 August–1 September 2004)* ed A Messac and J Renaud Paper AIAA-2004-4348
- [22] Egorov-Yegorov I N and Dulikravich G S 2005 Chemical composition design of superalloys for maximum stress, temperature and time-to-rupture using self-adapting response surface optimization *Mater. Manuf. Process.* **20** 569–90
- [23] Dulikravich G S and Egorov-Yegorov I N 2005 Robust optimization of concentrations of alloying elements in steel for maximum temperature, strength, time-to-rupture and minimum cost and weight, *ECCOMAS—Computational Methods for Coupled Problems in Science and Engineering (Fira, Santorini Island, Greece, 25–28 May 2005)* ed C Papadarakakis *et al*
- [24] Dulikravich G S and Egorov-Yegorov I N 2005 Design of alloy's concentrations for optimized strength, temperature, time-to-rupture, cost and weight *6th Int. Special Emphasis Symp. on Superalloys 718, 625, 706 and Derivatives (Pittsburgh, PA, 2–5 October 2005)* ed E A Loria (Pittsburgh, PA: TMS Publications) pp 419–28
- [25] Egorov I N 1998 Indirect optimization method on the basis of self-organization *Proc. Int. Conf. on Optimization Techniques and Applications (ICOTA'98) (Perth, Western Australia, July 1998)* (Perth: Curtin University of Technology) vol 2 pp 683–91
- [26] Tong S 1995 *Engineous User Manual* (Schenectady, NY: General Electric Corporate Research and Development Center) pp 1–292
- [27] Dulikravich G S, Martin T J, Dennis B H and Foster N F 1999 Multidisciplinary hybrid constrained GA optimization *EUROGEN'99—Evolutionary Algorithms in Engineering and Computer Science: Recent Advances and Industrial Applications (Jyvaskyla, Finland, 30 May–3 June)* ed K Miettinen *et al* (New York: Wiley) pp 231–60 Chapter 12

- [28] Dulikravich G S, Moral T J and Sahoo D 2005 A multi-objective evolutionary hybrid optimizer *EUROGEN 05—Evolutionary and Deterministic Methods for Design, Optimisation and Control with Applications to Industrial and Societal Problems (Munich, Germany, 12–14 September 2005)* ed R Schilling *et al*
- [29] Poloni C, Giurgevich A, Onesti L and Pediroda V 2000 Hybridization of a multi-objective genetic algorithm, neural network and classical optimizer for a complex design problem in fluid dynamics *Comput. Methods Appl. Mech. Eng.* **186** 403–20
- [30] Sahoo D and Dulikravich G S 2006 Evolutionary wavelet neural network for large scale function estimation in optimization *Proc. 11th AIAA/ISSMO Multidisciplinary Analysis and Optimization Conf. (Portsmouth, VA, 6–8 September 2006)* AIAA Paper AIAA-2006-6955
- [31] Wang H, Tan H and Li Y 2005 Multiple maxima of GFA in three adjacent eutectics in Zr-Cu-Al alloy system—A metallographic way to pinpoint the best glass forming alloys *Acta Mater.* **53** 2969–79
- [32] Tan H, Zhang Y, Ma D, Feng Y P and Li Y 2003 Optimum glass formation at off-eutectic composition and its relation to skewed eutectic coupled zone in the La based La-Al-(Cu,Ni) pseudo ternary system *Acta Mater.* **51** 4551–61
- [33] Sobol I M 1976 Uniformly distributed sequences with an additional uniform property *USSR Comput. Math. Math. Phys.* **16** 236–42
- [34] Moral R J and Dulikravich G S 2008 Multi-objective hybrid evolutionary optimization utilizing automatic algorithm switching *AIAA J.* **46** 673–700
- [35] Colaco M J, Sahoo D and Dulikravich G S 2007 A comparison of two methods for fitting high dimensional response surfaces *Proc. Int. Symp. on Inverse Problems, Design and Optimization (IPDO-2007) (Miami Beach, FL, 16–18 April 2007)* ed G S Dulikravich *et al*
- [36] Yegorov-Egorov I N and Dulikravich G S 2004 Inverse design of alloys for specified stress, temperature and time-to-rupture by using stochastic optimization *Proc. Int. Symp. on Inverse Problems, Design and Optimization—IPDO2004 (Rio de Janeiro, Brazil, 17–19 March)* ed M J Colaco *et al*
- [37] Martin T J and Dulikravich G S 2004 An implicit and explicit BEM sensitivity approach for thermo-structural optimization *Eng. Anal. Bound. Elem.* **28** 257–66
- [38] Pettersson F, Chakraborti N and Singh S B 2007 Neural networks analysis of steel plate processing augmented by multi-objective genetic algorithms *Steel Res. Int.* **78** 890–8
- [39] <http://www.calphad.com/jmatpro.html>
- [40] <http://www.crct.polymtl.ca/fact/>
- [41] Kumar A, Dulikravich G S and Egorov I N 2008 Titanium based alloy chemistry optimization for maximum strength, minimum weight and minimum cost using JMatPro and IOSO software *CD with Proc. from 2008 TMS Annual Meeting, Symp. on Materials Informatics: Enabling Integration of Modeling and Experiments in Materials Science (New Orleans, LA, 9–13 March 2008)* ed K Rajan